

Optical spectra and kinetic characteristics of radicals formed upon the photolysis of aqueous solutions of a $\text{FeOH}_{\text{aq}}^{2+}$ complex and phenol

I. P. Pozdnyakov,^a Yu. A. Sosedova,^b V. F. Plyusnin,^{a*} V. P. Grivin,^a
D. Yu. Vorob'ev,^b and N. M. Bazhin^a

^a*Institute of Chemical Kinetics and Combustion, Siberian Branch of the Russian Academy of Sciences,
3 ul. Institutskaya, 630090 Novosibirsk, Russian Federation.
Fax: +7 (383 2) 34 2350. E-mail: plyusnin@ns.kinetics.nsc.ru*

^b*Novosibirsk State University,
2 ul. Pirogova, 630090 Novosibirsk, Russian Federation*

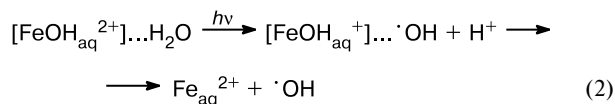
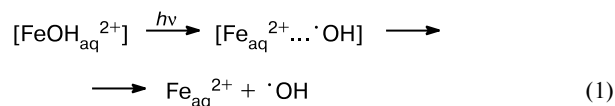
The nature, optical spectra, and kinetic characteristics were determined for intermediate radicals formed upon the photolysis of aqueous solutions of a $\text{FeOH}_{\text{aq}}^{2+}$ complex with phenol additives. The primary radical $\cdot\text{OH}$ reacts with phenol to form *ortho*- and *para*-isomers of the $\text{Ph}(\text{OH})_2\cdot$ radical. The $\text{Ph}(\text{OH})_2\cdot$ radical eliminates a water molecule to form a phenoxyl radical $\text{PhO}\cdot$. The latter disappears in the reactions with Fe^{III} complexes, recombination, and disproportionation. The final products of photochemical transformations were determined. Among them, *o*-quinone and diphenoquinones were identified.

Key words: photochemistry, aqueous solutions, iron complexes, phenol, radicals, laser flash photolysis, optical spectra, kinetics.

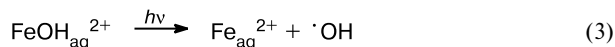
Phenol is a raw materials widely used in the chemical industry for syntheses of plastics, drugs, dyes, pesticides, preservatives, and surfactants.¹ Its world production exceeds 6 millions tons per year.² The active use of phenol contaminates the environment. The concentration of phenols in sewage can reach $100 \mu\text{g L}^{-1} \approx 10^{-6} \text{ mol L}^{-1}$.³ Phenol is very toxic (maximum allowable concentration $\approx 1 \mu\text{g L}^{-1} \approx 10^{-8} \text{ mol L}^{-1}$);⁴ therefore, the study of mechanisms of its degradation in natural water is of considerable interest from the ecological point of view. Photochemical processes can play an important role in the removal of contaminants from natural aqueous systems.^{5–7} A special attention is given to photoprocesses involving hydroxo complexes of Fe^{III} , whose photolysis affords an $\cdot\text{OH}$ radical, being one of the most active species in chemistry and capable of oxidizing almost all organic admixtures dissolved in water, including such hazardous substances as derivatives of the phenol series.^{8–10} The concentration of iron ions in natural water can approach $\sim 10^{-3} \text{ mol L}^{-1}$.^{11,12} In the absence of coordinating organic ligands, hydroxo complexes are the main forms of Fe^{III} in water with $\text{pH} < 5$, and the photochemistry of these complexes can exert a substantial effect on the balance of organic admixtures.^{6,13}

Among the Fe^{III} hydroxo complexes, the highest photochemical activity belongs to a complex $\text{FeOH}_{\text{aq}}^{2+}$, whose excitation is accompanied by the generation of an $\cdot\text{OH}$ radical with a high quantum yield ($\phi = 0.2$, $\lambda =$

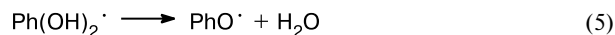
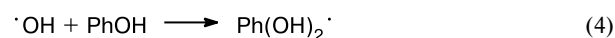
308 nm).^{14,15} The activation energy of formation of the $\cdot\text{OH}$ radical is only $\sim 10 \text{ kJ mol}^{-1}$,¹⁵ which explains its formation by the electron phototransfer to the Fe^{III} ion from both the outer-sphere hydroxide ion (reaction (1)) and outer-sphere water molecule (reaction (2)).¹⁵

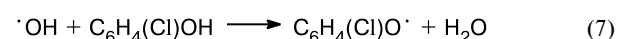
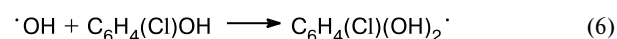
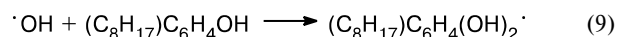
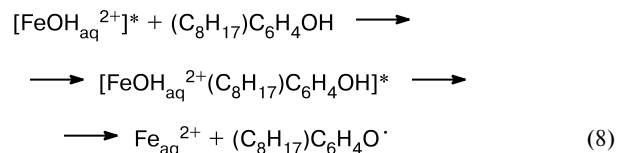


The formation of the $\cdot\text{OH}$ radical by the excitation of the $\text{FeOH}_{\text{aq}}^{2+}$ complex was confirmed in several studies on steady-state^{6,7,14} and flash photolyses^{10,15,16} using acceptors of the $\cdot\text{OH}$ radical. At least three mechanisms of degradation of phenol and its derivatives photoinduced by the $\text{FeOH}_{\text{aq}}^{2+}$ complex were proposed in the literature. These mechanisms include reactions (3)–(9).



Mechanism 1 (M1)

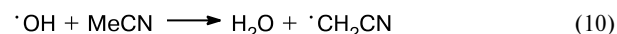


Mechanism 2 (M2)**Mechanism 3 (M3)**

Mechanism M1 was proposed by researchers¹⁶ who observed the generation of a radical $\text{PhO}\cdot$ during the photolysis of $\text{FeOH}_{\text{aq}}^{2+}$ in the presence of phenol. The time of formation and yield of the $\text{PhO}\cdot$ radical are independent of the initial phenol concentration in a wide range (10^{-4} – 10^{-2} mol L⁻¹). Similarly to the previously published work¹⁷ studying the flash radiolysis of aqueous solutions of phenol, it was assumed¹⁶ that the reaction of the $\cdot\text{OH}$ radical with phenol generated a radical $\text{Ph}(\text{OH})_2\cdot$, which, however, was not detected in that work.

When studying the photolysis of $\text{FeOH}_{\text{aq}}^{2+}$ in the presence of 4-chlorophenol (4-ClC₆H₄OH), the authors¹⁰ found the formation of two intermediates, whose overall quantum yield ($\phi = 0.071$, $\lambda = 355$ nm) coincided with the quantum yield of formation of the $\cdot\text{OH}$ radical ($\phi = 0.075$, $\lambda = 360$ nm).¹⁴ This coincidence and the data¹⁸ on the flash photolysis of aqueous solutions of 4-ClC₆H₄OH suggested¹⁰ the simultaneous formation of radicals $\text{C}_6\text{H}_4\text{Cl}(\text{OH})_2\cdot$ ($\phi = 0.056$) and $\text{C}_6\text{H}_4\text{Cl}(\text{O})\cdot$ ($\phi = 0.015$) in the reaction of the $\cdot\text{OH}$ radical with 4-ClC₆H₄OH (mechanism M2, reactions (6) and (7)).

The photochemistry of $\text{FeOH}_{\text{aq}}^{2+}$ in the presence of 4-octylphenol (OP) in aqueous-acetonitrile solutions was studied.⁸ A high concentration of acetonitrile (~ 2 mol L⁻¹) and rather high ($2.2 \cdot 10^7$ L mol⁻¹ s⁻¹)¹⁹ reaction rate



made it possible to assume⁸ that the $\cdot\text{OH}$ radical disappears completely upon this interaction. However, the flash photolysis of the $\text{FeOH}_{\text{aq}}^{2+}$ complex, under these conditions, results in the formation of an absorbance ($\lambda = 415$ nm) of a 4-octylphenoxyl radical ($(\text{C}_8\text{H}_{17})\text{C}_6\text{H}_4\text{O}\cdot \equiv \cdot\text{OPR}$). The observed rate constant of this process ($k_{\text{app}} = 1.5 \cdot 10^6$ s⁻¹) is independent of the OP concentration. Therefore, it was concluded that the $\cdot\text{CH}_2\text{CN}$ radical was not involved in the generation of the radical $\cdot\text{OPR}$. A hypothesis was advanced⁸ that an outer-sphere pair excited complex—OP molecule was formed followed by the electron transfer (mechanism M3, reaction (8)). This assumption seems doubtful, because the picosecond measurements demonstrated the short lifetime

($\tau \approx 55$ ps) of the excited complex $\text{FeOH}_{\text{aq}}^{2+}$.²⁰ When the OP concentration is $\sim 10^{-3}$ mol L⁻¹ as in the work,⁸ the fraction of excited complexes containing an OP molecule in the second coordination sphere does not exceed 0.1%.

The absence of a dependence of the time of $\cdot\text{OPR}$ formation on the OP concentration can be explained in terms of mechanism M1. The analysis shows that, for the reaction rate constant $k(\cdot\text{OH} + \text{OP}) \approx 5 \cdot 10^9$ L mol⁻¹ s⁻¹ and $[\text{OP}] \approx 10^{-3}$ mol L⁻¹, about 10% of the $\cdot\text{OH}$ radical can disappear in the reaction with OP. In fact, after a laser pulse, the absorbance at 350 nm increases⁸ with a rate threefold higher than the rate of $\cdot\text{OPR}$ formation ($\lambda = 415$ nm). It is known from the works on flash photolysis^{17,18,21} that adducts of $\cdot\text{OH}$ radical addition to phenols absorb at 300–350 nm. Thus, the absorbance at 350 nm can be attributed to the formation of a radical $(\text{C}_8\text{H}_{17})\text{C}_6\text{H}_4(\text{OH})_2\cdot$, which can produce the $\cdot\text{OPR}$ radical after the loss of a water molecule. In this case, the rate of $\cdot\text{OPR}$ formation is independent of the OP concentration.

Thus, the problem on the mechanism of reactions occurring during $\text{FeOH}_{\text{aq}}^{2+}$ photolysis in the presence of phenol and its derivatives remains unsolved. In this work, we studied the photochemistry of aqueous solutions of the $\text{FeOH}_{\text{aq}}^{2+}$ complex in the presence of phenol by laser flash photolysis, optical spectroscopy, and HPLC. The main purpose was to determine the nature of the reactions and spectroscopic and kinetic parameters of intermediate species.

Experimental

A laser flash photolysis technique including an excimeric XeCl laser (308 nm) with a pulse duration of 15 ns and an average pulse energy of 20 mJ was used.²² All measurements were carried out in a cell with an optical path length of 1 cm. A radiation from an XeCl laser or a mercury lamp (DRSh-500) with an array of glass filters to separate particular lines was used for steady-state photolysis. Electronic absorption spectra were recorded on a Hewlett Packard HP 8453 spectrophotometer. The final products of photochemical reactions were analyzed on a Spectra Physics SP8800-20 HPLC chromatograph with a UV detector (220 nm). A specially developed program was used for the numerical simulation of kinetic curves to solve a system of differential equations.

Experiments were carried out in deoxygenated aqueous solutions with pH ≈ 3 . To remove oxygen, nitrogen or argon was passed through solutions for 20 min. At pH ≈ 3 , $\sim 85\%$ of Fe^{III} ions exist as a complex $\text{FeOH}_{\text{aq}}^{2+}$ and 15% exist as $\text{Fe}_{\text{aq}}^{3+}$.¹⁴ The molar absorption coefficient at 308 nm for $\text{FeOH}_{\text{aq}}^{2+}$ (1880 L mol⁻¹ cm⁻¹) is much higher than that for $\text{Fe}_{\text{aq}}^{3+}$ (64 L mol⁻¹ cm⁻¹).^{14,23} Therefore, the main absorbing and photoactive species was the complex $\text{FeOH}_{\text{aq}}^{2+}$ (standard concentration $4 \cdot 10^{-4}$ mol L⁻¹). Salt $\text{Fe}(\text{ClO}_4)_3 \cdot \text{H}_2\text{O}$ (Aldrich) and twice-distilled water were used to prepare solutions. Phenol (Aldrich) was analyzed for the presence of admixtures by HPLC and used without additional purification. Its aqueous solutions do not absorb at 308 nm and are resistant toward laser radiation.

Results and Discussion

Laser flash photolysis of solutions of $\text{FeOH}_{\text{aq}}^{2+}$ with phenol additives. The pulse photoexcitation of aqueous solutions of $\text{FeOH}_{\text{aq}}^{2+}$ results in the disappearance of the absorbance of this complex, and no signals of an intermediate absorbance appear. In aqueous solutions of $\text{FeOH}_{\text{aq}}^{2+}$ containing phenol, an intermediate absorbance appears in the spectrum after a laser pulse. The kinetics of changes in this absorbance at 335 and 400 nm for a low phenol concentration ($4.5 \cdot 10^{-5} \text{ mol L}^{-1}$) is shown in Fig. 1. After a laser pulse, the absorbance at 335 nm decreases due to the disappearance of the absorbance of $\text{FeOH}_{\text{aq}}^{2+}$ (the kinetics at the zero phenol concentration is presented in Fig. 1 for comparison). The molar absorption coefficient of $\text{FeOH}_{\text{aq}}^{2+}$ at 335 nm is equal to $1085 \text{ L mol}^{-1} \text{ cm}^{-1}$. After $\sim 2 \mu\text{s}$, a new absorbance is formed at this wavelength and begins to disappear in $3 \mu\text{s}$. No absorbance decrease at 400 nm can be detected, because for $\text{FeOH}_{\text{aq}}^{2+}$ $\epsilon^{400} = 85 \text{ L mol}^{-1} \text{ cm}^{-1}$. The intermediate absorbance at this wavelength begins to increase from zero and passes through a maximum in the region about $20 \mu\text{s}$ at a given phenol concentration (see Fig. 1).

An increase in the phenol concentration accelerates the formation of the intermediate absorbance. The ki-

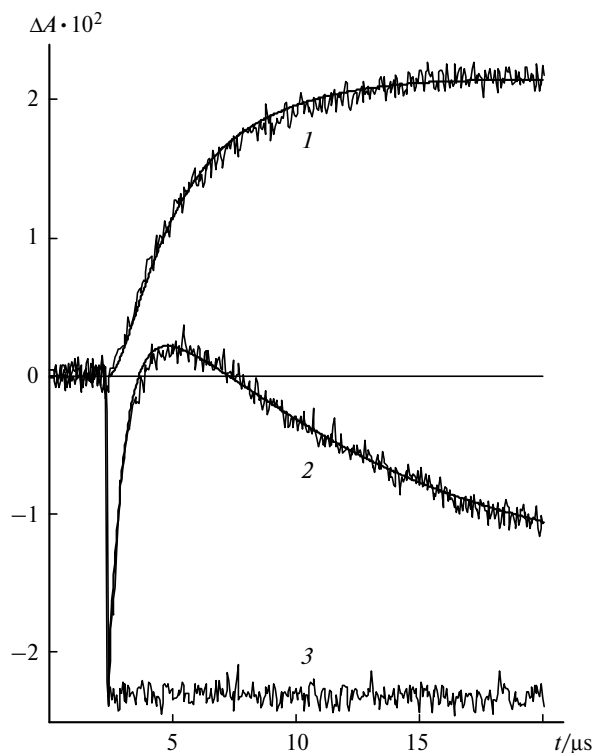


Fig. 1. Kinetic curves of the changes in absorbance (ΔA) upon the flash photolysis of solutions of $\text{FeOH}_{\text{aq}}^{2+}$: 1 and 2, detection wavelengths are 400 and 335 nm, respectively, $[\text{PhOH}] = 4.5 \cdot 10^{-5} \text{ mol L}^{-1}$; 3, 335 nm, $[\text{PhOH}] = 0 \text{ mol L}^{-1}$. Smooth curves are the calculation by the scheme of reactions (18)–(26) with the parameters given in Tables 1 and 2.

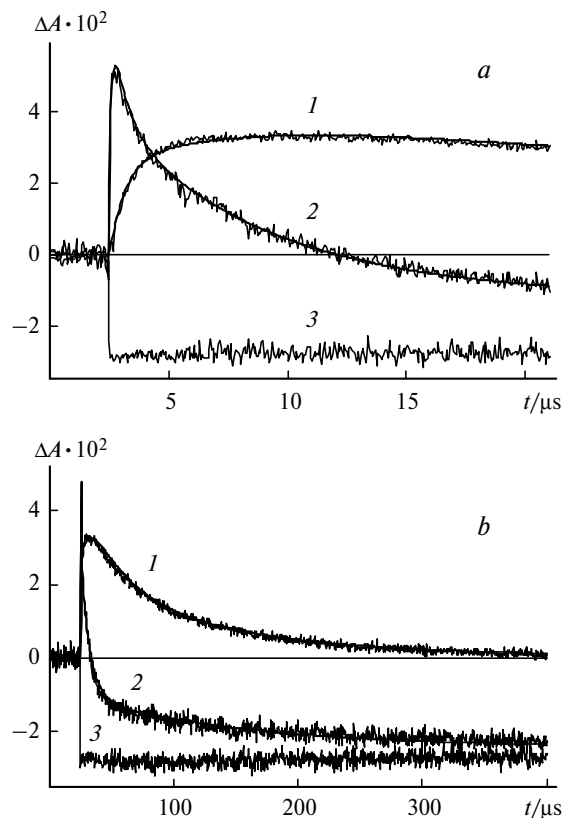


Fig. 2. Kinetic curves of the changes in absorbance (ΔA) upon the flash photolysis of solutions of $\text{FeOH}_{\text{aq}}^{2+}$ with different (a, b) time sweeps: 1 and 2, detection wavelengths are 400 and 335 nm, respectively, $[\text{PhOH}] = 1.1 \cdot 10^{-3} \text{ mol L}^{-1}$; 3, 335 nm, $[\text{PhOH}] = 0 \text{ mol L}^{-1}$. Smooth curves are the calculation by the scheme of reactions (18)–(26) with the parameters given in Tables 1 and 2.

netic curves at the same wavelengths at a higher phenol concentration ($1.1 \cdot 10^{-3} \text{ mol L}^{-1}$) are presented in Fig. 2. In this case, the absorbance at 335 nm appears within the time $< 50 \text{ ns}$, and only its disappearance can be detected. The time sweep of $400 \mu\text{s}$ distinctly shows that this absorbance decreases in two steps with substantially different rates. The time of absorbance formation at 400 nm also decreases with an increase in the phenol content, although to a much lower extent. Even at a high phenol concentration, the time of its appearance is several microseconds yet. The absorbance at 400 nm continues increasing even when the absorbance at 335 nm is already decreasing.

The changes in the intermediate spectra in time are shown in Fig. 3. When plotting these spectra, we took into account the initial absorbance decrease in the region of the absorption band of the $\text{FeOH}_{\text{aq}}^{2+}$ complex. For a phenol concentration of $5.9 \cdot 10^{-5} \text{ mol L}^{-1}$, a band with a maximum at 335 nm and two weaker bands at 380 and 400 nm are formed within $0.8 \mu\text{s}$. The intensities of two latter bands increase simultaneously with time and reach a maximum after $\sim 15 \mu\text{s}$. Much later, the absorbance at these wavelengths decreases to zero, and the absorbance

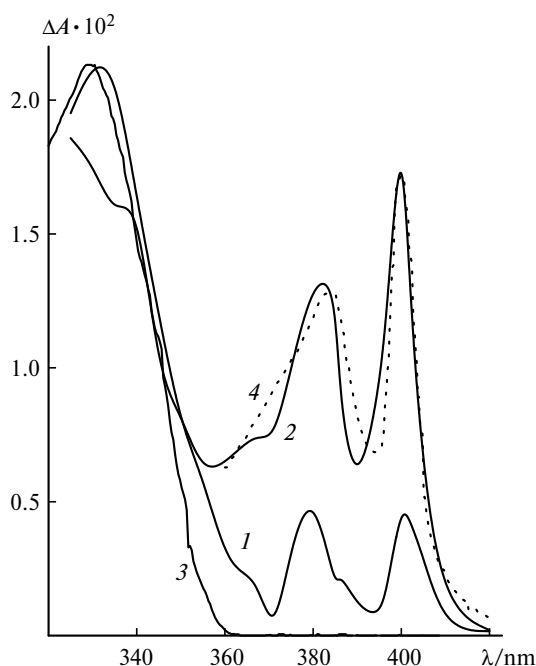


Fig. 3. Intermediate absorption spectra (ΔA) upon the flash photolysis of a solution of the $\text{FeOH}_{\text{aq}}^{2+}$ complex in the presence of phenol ($5.9 \cdot 10^{-5} \text{ mol L}^{-1}$): 1 and 2, spectra obtained 0.8 and 2.4 μs after a laser pulse; 3 and 4, earlier published spectra of the radicals $\text{Ph}(\text{OH})_2^\cdot$ ¹⁷ and PhO^\cdot ²⁶, respectively.

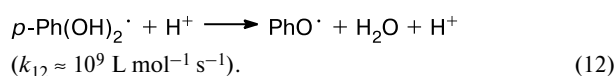
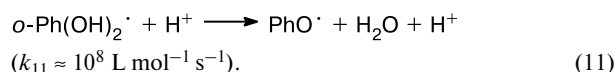
at 335 nm decreases due to the disappearance of the absorbance of the $\text{FeOH}_{\text{aq}}^{2+}$ complex.

It is known from the studies on flash radiolysis²¹ that the reaction of an $^\cdot\text{OH}$ radical with aromatic molecules (ArH) predominantly affords the corresponding hydroxycyclohexadienyl radical ($\text{Ar}(\cdot\text{OH})\text{H}$). The absorption maximum of the most part of adducts of the $^\cdot\text{OH}$ radical to benzene derivatives appears at 310–350 nm^{17,18,21} (320–330 nm for a radical $\text{Ph}(\text{OH})_2^\cdot$ ^{17,21}). These data suggest that the primary intermediate absorption band with a maximum at 335 nm corresponds to the radical $\text{Ph}(\text{OH})_2^\cdot$, whose spectrum is presented in Fig. 3 (see Ref. 17).

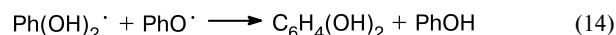
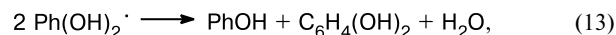
The $\text{Ph}(\text{OH})_2^\cdot$ radical eliminates a water molecule to form a radical PhO^\cdot , and this process is accelerated in the presence of acids and bases.^{17,24} The phenoxyl radical has a characteristic spectrum containing two absorption bands with maxima at 380 and 400 nm. The optical spectrum of this species has been detected for the first time when aqueous solutions of phenol were studied by flash photolysis.²⁵ Further, the spectra of substituted phenoxyl radicals containing absorption bands at 370–430 nm were obtained. These absorption bands are close in shape and position to the bands in the spectrum of the unsubstituted phenoxyl radical.^{18,26–28} The spectrum of the PhO^\cdot radical²⁶ (see Fig. 3, curve 4) agrees well with that obtained by us. Thus, the laser flash photolysis data indicate the formation of radicals $\text{Ph}(\text{OH})_2^\cdot$ and PhO^\cdot upon the

excitation of the $\text{FeOH}_{\text{aq}}^{2+}$ complex in the presence of phenol.

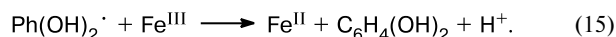
Mechanism of formation and reactions of the radical $\text{Ph}(\text{OH})_2^\cdot$. An $^\cdot\text{OH}$ radical can add to the double bond of a phenol molecule in four possible positions. For the γ -radiolysis of aqueous solutions of phenol, the predominant formation of *ortho*- and *para*-isomers of the $\text{Ph}(\text{OH})_2^\cdot$ radical was observed (48 and 36%, respectively, of the number of disappeared phenol molecules).^{10,24} In an acidic medium (pH 3–4), the main channel for the decay of these isomers is the acid-catalyzed elimination of a water molecule to form a phenoxyl radical²⁴



Two time intervals with significantly different rates of disappearance of the absorption band at 335 nm also indicate the formation of two isomers of the $\text{Ph}(\text{OH})_2^\cdot$ radical. This is well seen for high phenol concentrations ($\sim 10^{-3} \text{ mol L}^{-1}$) and in a time sweep of 400 μs (see Fig. 2, b). Along with reactions (11) and (12), additional channels of disappearance of the primary radical $\text{Ph}(\text{OH})_2^\cdot$ can be the following disproportionation processes



and the reaction



The rate constant of disappearance of the $\text{C}_6\text{H}_4(\text{Cl})(\text{OH})_2^\cdot$ radical in the second-order reaction is $k_{13} = 3 \cdot 10^8 \text{ L mol}^{-1} \text{ s}^{-1}$.²⁹ Under the assumption that these constants for the radicals $\text{Ph}(\text{OH})_2^\cdot$ and $\text{C}_6\text{H}_4(\text{Cl})(\text{OH})_2^\cdot$ are close, the apparent rate constant of $\text{Ph}(\text{OH})_2^\cdot$ radical disappearance in reaction (13) ($k_{\text{app}} = k_{13}[\text{Ph}(\text{OH})_2^\cdot]_0 \approx 6 \cdot 10^3 \text{ s}^{-1}$) is much lower than the apparent rate constants of reactions (11) and (12) at pH 3 ($k_{\text{app}} = k_{11}[\text{H}^+] \approx 10^5 \text{ s}^{-1}$, $k_{\text{app}} = k_{12}[\text{H}^+] \approx 10^6 \text{ s}^{-1}$). The variation of the initial concentration of Fe^{III} has virtually no effect on the rate of $\text{Ph}(\text{OH})_2^\cdot$ radical disappearance, indicating a low rate constant of reaction (15). At the same time, reaction (14) can play a substantial role in the disappearance of the $\text{Ph}(\text{OH})_2^\cdot$ radical^{18,30} due to a high redox potential of the phenoxyl radical ($E_0(\text{PhO}^\cdot, \text{H}^+/\text{PhOH}) = 1.33 \text{ V}$),³¹ and the contribution of this reaction will be considered below.

Mechanism of formation and reactions of the radical PhO^\cdot . The apparent rate constant of formation of the phenoxyl radical absorbance (at $\lambda = 400 \text{ nm}$) increases

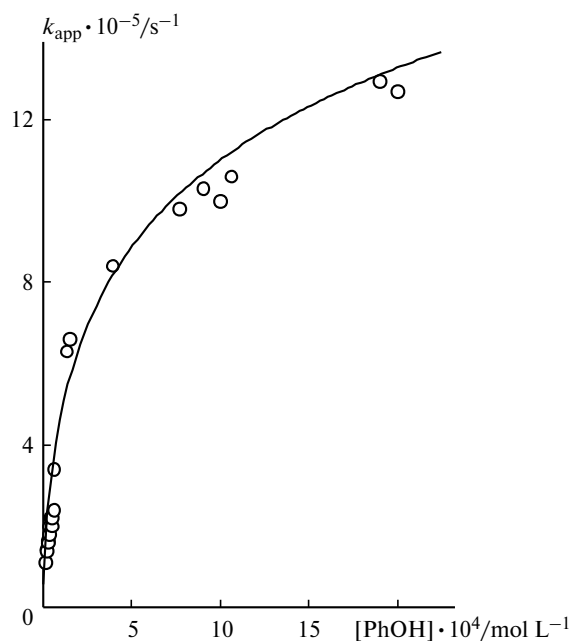


Fig. 4. Apparent rate constant of absorbance formation of the PhO^\bullet radicals (400 nm) vs. initial phenol concentration. Curve is the approximation of the experimental data (points) by formula (16).

nonlinearly with an increase in the phenol concentration and reaches a stationary value at a concentration higher than $10^{-3} \text{ mol L}^{-1}$ (in this region, $k_{\text{app}} \approx 10^6 \text{ s}^{-1}$ (Fig. 4)). These results exclude a possibility of formation of the phenoxyl radical *via* mechanism M3, because, in this case, k_{app} should be determined by the lifetime of an excited complex $[\text{FeOH}_{\text{aq}}^{2+} \dots \text{PhOH}]^*$ and would not depend on the phenol concentration. Mechanism M2 is also highly improbable because of the nonlinear dependence of k_{app} on the phenol concentration. The upper estimate of the bimolecular rate constant of elimination of an H atom from a phenol molecule by an $^\bullet\text{OH}$ radical (k_{bim}) obtained using k_{app} gives $k_{\text{bim}} = k_{\text{app}}/[\text{PhOH}] \leq 10^9 \text{ L mol}^{-1} \text{ s}^{-1}$. The reaction rate constant of addition of the $^\bullet\text{OH}$ radical to the phenol molecule is by an order of magnitude higher^{17,26,32} and, therefore, the elimination cannot contribute substantially to the formation of the PhO^\bullet radical.

It can be noted that the obtained experimental data are well explained in the framework of mechanism M1. An analysis shows that the dependence of the apparent rate constant of PhO^\bullet radical formation on the phenol concentration in the approximation of pseudo-first order reactions ($[\text{PhOH}], [\text{H}^+] \gg [\text{Ph}(\text{OH})_2^\bullet], [\text{PhO}^\bullet]$) is determined by the expression

$$k_{\text{app}} = \frac{k_m k_{\text{bim}} [\text{PhOH}]}{k_m - k_{\text{bim}} [\text{PhOH}]} \ln \frac{k_m}{k_{\text{bim}} [\text{PhOH}]}, \quad (16)$$

where k_{bim} is the rate constant of $^\bullet\text{OH}$ radical addition to the phenol molecule, and k_m is the pseudo-monomolecular constant of the reaction $\text{Ph}(\text{OH})_2^\bullet \rightarrow \text{PhO}^\bullet$ (at a

given concentration of H^+). At low phenol concentrations ($k_{\text{bim}}[\text{PhOH}] \ll k_m$), a dependence $k_{\text{app}} \sim [\text{PhOH}]$ close to linear is observed. In this case, the rate of PhO^\bullet formation is limited by the rate of formation of the primary radical $\text{Ph}(\text{OH})_2^\bullet$. In the opposite case ($k_{\text{bim}}[\text{PhOH}] \gg k_m$), the rate of $\text{Ph}(\text{OH})_2^\bullet$ decomposition is rate-determining, and an increase in k_{app} with an increase in the phenol concentration is substantially inhibited. The solid line in Fig. 4 shows a satisfactory approximation of the experimental data by formula (16) with the values $k_{\text{bim}} \approx 6.7 \cdot 10^9 \text{ L mol}^{-1} \text{ s}^{-1}$ and $k_m \approx 3.6 \cdot 10^5 \text{ s}^{-1}$. These parameters agree well with the results of precision calculations of the kinetic curves in the framework of the proposed kinetic model.

To determine the nature of reactions in which the secondary PhO^\bullet radical disappears, one can determine the dependences of k_{app} on the amplitude of the signal (variation of the laser pulse intensity) and on the phenol and Fe^{III} ion concentrations using the kinetics of disappearance of the absorbance of this radical (400 nm). As shown in Fig. 5, *a*, the plot $k_{\text{app}} \sim \Delta A(400 \text{ nm})$ is linear with a non-zero intercept. This section increases with an increase in the Fe^{III} concentration (Fig. 5, *b*). The apparent rate constant of PhO^\bullet radical disappearance is independent of the phenol concentration.

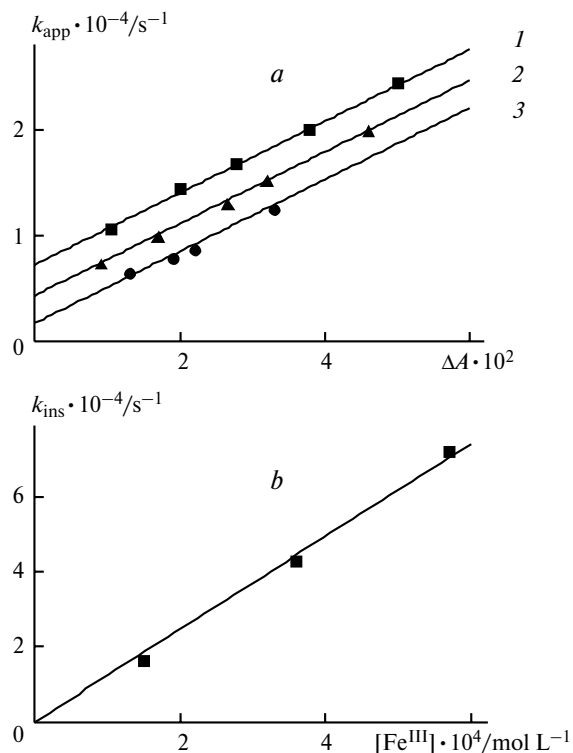
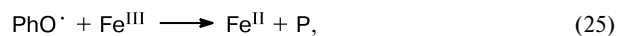
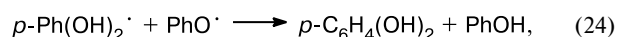
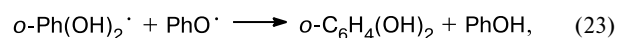
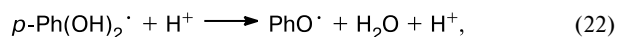
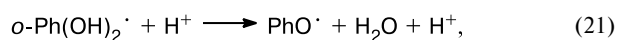
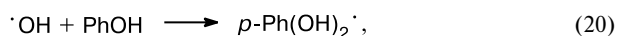
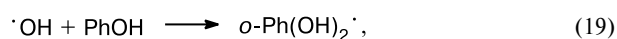
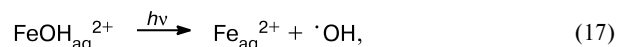


Fig. 5. Dependence of the apparent rate constant of the disappearance of absorbance of the PhO^\bullet radical (400 nm) on the signal amplitude (*a*) at $[\text{Fe}^{\text{III}}] \cdot 10^4 = 1.6$ (1), 3.5 (2), and 5.7 mol L^{-1} (3) and the dependence of the intercept in the plot *a* on the Fe^{III} concentration (*b*).

The data obtained show that the PhO^\bullet radical disappears in the second-order reaction and in the reaction with the Fe^{III} complexes. The slope ratio of the straight lines in Fig. 5, *a* makes it possible to determine $2k/\epsilon = 3.3 \cdot 10^5 \text{ cm s}^{-1}$ for the second-order reaction (k is the rate constant of the second-order reaction, and ϵ is the molar absorption coefficient of the absorption band of the PhO^\bullet radical at 400 nm). The slope of the straight line in Fig. 5, *b* determines the rate constant of the reaction of PhO^\bullet with the Fe^{III} complexes ($k = 1.2 \cdot 10^7 \text{ L mol}^{-1} \text{ s}^{-1}$).

Kinetic scheme of reactions. Based on the results of the present study, we can propose the following scheme of reactions for the photolysis of $\text{FeOH}_{\text{aq}}^{2+}$ in the presence of phenol:



The pairs of reactions (19), (20) and (21), (22) correspond to processes involving the *ortho*- and *para*-isomers of the $\text{Ph}(\text{OH})_2^\bullet$ radical.

In terms of the scheme of reactions (17)–(26), we calculated the kinetic curves by the numerical solution of differential equations by the Runge–Kutt method of the fourth order. The kinetic curves at 335 and 400 nm were simultaneously calculated and fitted to the experimental curves. The initial concentration of the $\cdot\text{OH}$ radical (determined from the absorbance decrease at 335 nm for solutions of $\text{FeOH}_{\text{aq}}^{2+}$ without phenol), molar absorption coefficient of the $\text{FeOH}_{\text{aq}}^{2+}$ complex at 335 nm, and rate constants of reactions (18)–(22) and (25) were used as nonvariable parameters. The molar absorption coefficients of the radicals $\text{Ph}(\text{OH})_2^\bullet$ (335 nm) and PhO^\bullet (400 nm), rate constants of reactions (23), (24), and (26), and molar absorption coefficient at 335 nm of the product P formed in reaction (25) were varied.

The best agreement between the experimental and calculated curves was achieved when the molar absorption coefficients of the radicals $o\text{-Ph}(\text{OH})_2^\bullet$, $p\text{-Ph}(\text{OH})_2^\bullet$, and PhO^\bullet close to published values (Table 1) were used. The value of the rate constant of the reaction of the $\cdot\text{OH}$ radical with phenol obtained in radiation chemical ex-

Table 1. Molar absorption coefficients (ϵ) of absorption bands of intermediate species used in the calculation of the kinetic curves

Species	λ/nm	$\epsilon \cdot 10^{-3}/\text{L mol}^{-1} \text{ cm}^{-1}$		Refs
		Calculation	Literature data	
$p\text{-Ph}(\text{OH})_2^\bullet$	335	$3.1 \pm 0.3^*$	4.4 ± 0.8	17
$o\text{-Ph}(\text{OH})_2^\bullet$	335	$3.7 \pm 0.9^*$	4.4 ± 0.8	17
PhO^\bullet	400	2.1 ± 0.3	2.2 ± 0.2	17, 26
P**	335	2.0 ± 0.6	—	

* $\epsilon^{335} = (k_{19}\epsilon_o^{335} + k_{20}\epsilon_p^{335})/(k_{19} + k_{20}) = (3.4 \pm 0.7) \cdot 10^3 \text{ L mol}^{-1} \text{ cm}^{-1}$.

** P is the product formed in reaction (25).

Table 2. Reaction rate constants (k) used for the calculation of the kinetic curves

Reaction	$k \cdot 10^{-9}/\text{L mol}^{-1} \text{ s}^{-1}$		Refs
	Calculation	Literature data	
18	5.5^*	5.5	19
19	8^*	14^{**}	17, 32
20	6^*	14^{**}	17, 32
21	1^*	1	24
22	0.1^*	0.1	24
23, 24	2.9 ± 0.6	—	
25	0.012^*	—	
26	0.49 ± 0.17	0.30	26
		0.79	33
		0.54	34

* Nonvariable parameter.

** $k = k_{19} + k_{20}$.

periments ($1.4 \cdot 10^{10} \text{ L mol}^{-1} \text{ s}^{-1}$)¹⁷) was distributed between the isomers. For the reactions of decomposition of the $\text{Ph}(\text{OH})_2^\bullet$ radical isomers, the rate constants coincided with the published data (Table 2). As can be seen from Figs 1 and 2, the calculated curves satisfactorily correspond to the experimental kinetic curves in a wide interval of phenol concentrations. This agreement confirms that the photochemical transformations in the Fe^{III} –phenol system was adequately described in terms of mechanism M1.

Final products of radical reactions. Regardless of the nature of phenoxyl radicals and a method for their generation (steady-state photolysis,³⁵ flash photolysis in the presence of azide,³⁶ photochemical²⁷ and enzymatic³⁷ oxidation), in the absence of strong oxidants, the radicals disappear in recombination to form dimeric products (predominantly, dihydroxybiphenyls). The final products of reactions (13) and (14) of the $\text{Ph}(\text{OH})_2^\bullet$ radical are dihydroxybenzenes, viz., catechol and hydroquinone.^{18,30,38–41}

In the presence of oxidants (oxygen, transition metal ions), both the $\text{Ph}(\text{OH})_2^\bullet$ and PhO^\bullet radicals and products of their reactions (dihydroxybiphenyls and dihydroxy-

benzenes) are oxidized to the corresponding quinones and ring opening products.^{27,38,42–47}

To determine the final products of phenol photo-degradation in the presence of $\text{FeOH}_{\text{aq}}^{2+}$, we carried out the steady-state photolysis (308 nm) of aqueous solutions of the complex with phenol additives followed by spectrophotometric and chromatographic analyses. It was found that a new absorption band formed slowly at 400 nm (Fig. 6, *a*) after irradiation was stopped. The rate of its formation depends on the initial concentration of the Fe^{III} ions (Fig. 6, *b*). The molar absorption coefficient of this band considerably exceeds that of the band of $\text{FeOH}_{\text{aq}}^{2+}$ (300 nm), because an increase in the absorbance at 400 nm induces a slight change in the absorbance at 300 nm.

It is known^{42,44} that diphenoquinones are characterized by the absorption band with a maximum at 400 nm with molar extinction coefficients of $\sim 10^4$ – 10^5 $\text{L mol}^{-1} \text{cm}^{-1}$ ($\epsilon^{418} = 9.0 \cdot 10^4$ $\text{L mol}^{-1} \text{cm}^{-1}$ for 3,3',5,5'-tetramethyldiphenoquinone⁴⁴). Thus, the band at 400 nm can be related to the formation of dipheno-

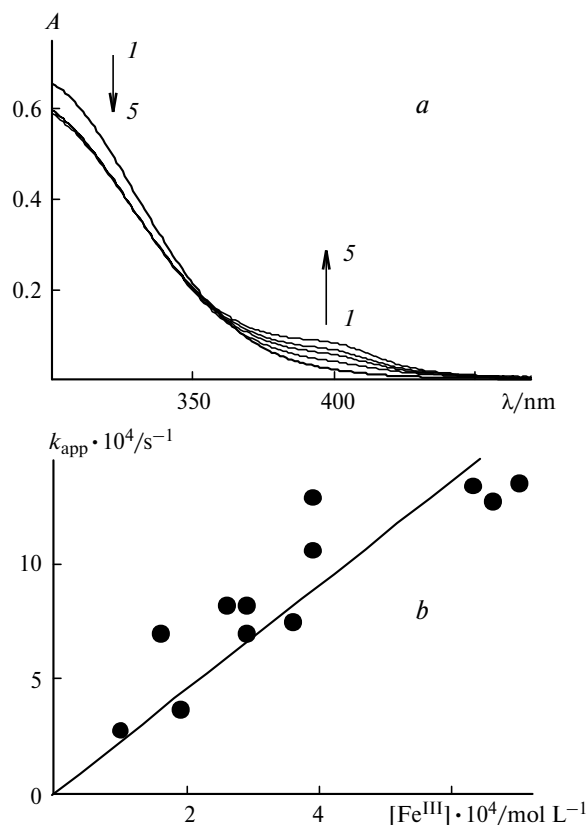


Fig. 6. *a*. Change in the optical spectrum (*A*) of a solution of the $\text{FeOH}_{\text{aq}}^{2+}$ complex in the presence of phenol ($1.07 \cdot 10^{-3}$ mol L^{-1}) after irradiation (XeCl laser, 308 nm, 600 mJ over 15 s, solution volume 3 mL): spectrum before irradiation (*I*); spectra 4 (2), 9 (3), 15 (4), and 50 min (5) after irradiation. *b*. Dependence of k_{app} of the appearance of a new absorption band at 400 nm on the Fe^{III} concentration.

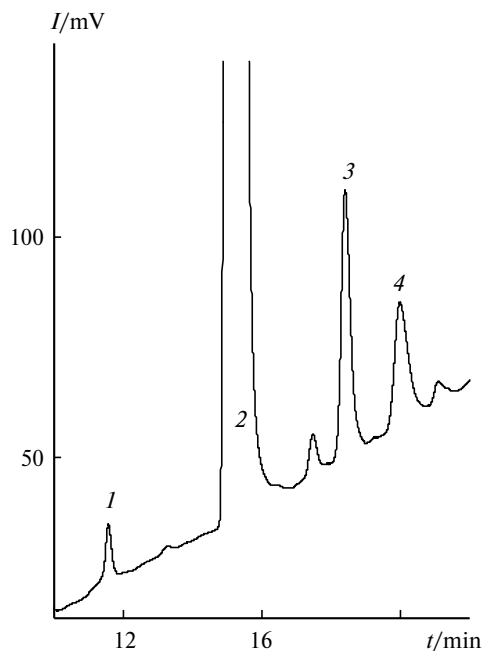


Fig. 7. Chromatogram of the photolysis products of aqueous solutions of the $\text{FeOH}_{\text{aq}}^{2+}$ complex in the presence of phenol ($1.4 \cdot 10^{-3}$ mol L^{-1}): 1, *o*-quinone; 2, phenol; 3 and 4, dimeric products (diphenoquinones). Photolysis (XeCl laser, 308 nm, 4 J over 100 s, volume 3 mL) followed by extraction with CH_2Cl_2 , distillation of an extractant, and dissolution of a dry residue in ethanol. Column 4×150 mm, Lichrospher RP-18, 5 μm , UV detector (220 nm); solvents: *A*, water; *B*, acetonitrile, linear gradient: 0 min — 0% *B*, 20 min — 85% *B*; flow rate 1.0 mL min^{-1} .

quinones in the oxidation of dihydroxybiphenyls (recombination products of two phenoxyl radicals) with the Fe^{III} ions. This assumption agrees with the results of chromatographic analysis of irradiated solutions (Fig. 7). The highest intensity belongs to peaks 3 and 4 with a longer elution time. These peaks can be assigned to isomeric diphenoquinones.

Dihydroxybenzenes (catechol and hydroquinone) formed in reactions (23) and (24) can easily be oxidized to the corresponding quinones.^{42–47} The elution time of peak 1 coincides with that of *o*-quinone obtained by the chemical oxidation of catechol with the Fe^{III} ions. In the framework of the above-proposed scheme of reactions, we calculated the yields of hydroquinone and catechol in reactions (23) and (24) using the tabulated (Table 2) rate constants of reactions (18)–(26). These calculations showed that only an insignificant amount of *ortho*- and *para*-isomers of the $\text{Ph}(\text{OH})_2^{\cdot}$ radical (~ 10 and 1%, respectively) can be involved in reactions (23) and (24). The low yield of hydroquinone in reaction (23) explains the absence of a chromatographic peak of *p*-quinone.

Thus, precision measurements of the kinetics of reactions of radicals appeared by the photolysis of aqueous solutions of $\text{FeOH}_{\text{aq}}^{2+}$ and phenol were performed. The

optical spectrum and kinetic parameters of the $\text{Ph}(\text{OH})_2^\cdot$ radical generated by the reaction of the $^\cdot\text{OH}$ radical with phenol were obtained. The data obtained made it possible to propose the scheme of photochemical degradation of phenol. It was shown that two isomers of the $\text{Ph}(\text{OH})_2^\cdot$ radical were formed and transformed into the phenoxyl radical PhO^\cdot with water molecule elimination. The molar absorption coefficients and rate constants of the reactions of radical species were determined by the comparison of the calculated and experimental kinetic curves. *o*-Quinone and diphenoquinones were identified among the final products of photochemical transformations.

This work was financially supported by the Russian Foundation for Basic Research (Project Nos. 02-03-32797, 03-03-33314, and 03-03-39008GFEN) and the Ministry of Education of the Russian Federation (Program "Universities of Russia," Grant UR.05.01.002).

References

- G. D. Kharlampovich and Yu. V. Churkin, *Fenoly [Phenols]*, Khimiya, Moscow, 1974, 328 pp. (in Russian).
- G. I. Panov and A. S. Kharitonov, *Ros. Khim. Zh.*, 2000, **44**, 7 [*Mendeleev Chem. J.*, 2000, **44** (Engl. Transl.)].
- E. M. Thurman, *Organic Geochemistry of Natural Waters*, Martinus Nijhoff, Dr W. Junk Publisher, Kluwer Academic Publishers Group, Dordrecht—Boston—Lancaster, 1985, 610 pp.
- Predel'no dopustimye kontsentratsii khimicheskikh veshchestv v okruzhayushchei srede [Maximum Allowable Concentrations of Chemical Compounds in the Environment]*, Eds G. P. Bospamyatnov and Yu. A. Krotov, Khimiya, Leningrad, 1985, 528 pp. (in Russian).
- The Handbook of Environmental Chemistry*, Ed. P. Boule, **2**, Part L: *Environmental Photochemistry*, Springer, Berlin, 1999.
- B. S. Faust and J. Hoigne, *Atmospheric Environment*, 1990, **24A**, 79.
- W. Feng and D. Nansheng, *Chemosphere*, 2000, **41**, 1137.
- N. Brand, G. Mailhot, M. Sarakha, and M. Bolte, *J. Photochem. Photobiol. A: Chem.*, 2000, **135**, 221.
- N. Brand, G. Mailhot, and M. Bolte, *Environ. Sci. Technol.*, 1998, **32**, 2715.
- P. Mazellier, G. Mailhot, and M. Bolte, *New J. Chem.*, 1999, **23**, 133.
- V. V. Dobrovol'skii, *Osnovy biogeokhimii [Foundations of Biogeochemistry]*, Vysshaya Shkola, Moscow, 1998, p. 93 (in Russian).
- A. I. Perel'man, *Geokhimiya [Geochemistry]*, Vysshaya Shkola, Moscow, 1989, p. 444 (in Russian).
- Y. Zuo and J. Holdne, *Environ. Sci. Technol.*, 1992, **26**, 1014.
- H. J. Benkelberg and P. Warnek, *J. Phys. Chem.*, 1995, **99**, 5214.
- I. P. Pozdnyakov, E. M. Glebov, V. F. Plyusnin, V. P. Grivin, Y. V. Ivanov, D. Y. Vorobyev, and N. M. Bazhin, *Pure Appl. Chem.*, 2000, **72**, 2187.
- V. A. Nadtochenko and J. Kiwi, *Inorg. Chem.*, 1998, **37**, 5233.
- E. J. Land and M. Ebert, *Trans. Far. Soc.*, 1967, **63**, 1181.
- U. Stafford, K. A. Gray, and P. V. Kamat, *J. Phys. Chem.*, 1994, **98**, 6343.
- G. V. Buxton, C. L. Greenstock, W. P. Helman, and A. B. Ross, *J. Phys. Chem. Ref. Data*, 1988, **17**, 513.
- T. Okazaki, N. Hirota, and M. Terazima, *J. Phys. Chem. A*, 1997, **101**, 650.
- L. M. Dorfman, I. A. Taub, and R. E. Buhler, *J. Chem. Phys.*, 1962, **36**, 3051.
- V. P. Grivin, I. V. Khmelinski, V. F. Plyusnin, I. I. Blinov, and K. P. Balashev, *J. Photochem. Photobiol. A: Chem.*, 1990, **51**, 167.
- F. S. Dainton and D. G. L. James, *Trans. Faraday Soc.*, 1958, **54**, 649.
- N. V. Raghavan and S. Steenken, *J. Am. Chem. Soc.*, 1980, **102**, 3495.
- E. J. Land, G. Porter, and E. Strachan, *Trans. Faraday Soc.*, 1961, **57**, 1885.
- R. J. Field, N. V. Raghavan, and J. G. Drummer, *J. Phys. Chem.*, 1982, **86**, 2443.
- M. Sarakha, M. Bolte, and H. D. Burrows, *J. Photochem. Photobiol. A: Chem.*, 1997, **107**, 101.
- G. Dobson and L. I. Grossweiner, *Trans. Faraday Soc.*, 1965, **61**, 708.
- N. Getoff and S. Solar, *Radiat. Phys. Chem.*, 1988, **31**, 121.
- S. Schmid, P. Krajnik, R. M. Quint, and S. Solar, *Radiat. Phys. Chem.*, 1997, **50**, 493.
- P. Wardman, *J. Phys. Chem. Ref. Data*, 1989, **18**, 1637.
- M. Roder, L. Wojnarovits, G. Foldiak, S. S. Emmi, G. Beggiato, and M. D'Angelantonio, *Radiat. Phys. Chem.*, 1999, **54**, 475.
- E. J. Land and G. Porter, *Trans. Faraday Soc.*, 1963, **59**, 2016.
- L. I. Grossweiner and E. F. Zwicker, *J. Chem. Phys.*, 1961, **34**, 1411.
- H.-J. Joschek and S. I. Miller, *J. Am. Chem. Soc.*, 1966, **88**, 3273.
- M. Ye, R. H. Schuler, *J. Phys. Chem.*, 1989, **93**, 1898.
- E. Laurenti, E. Ghibaudi, G. Todaro, and R. P. Ferrari, *J. Inorg. Biochem.*, 2002, **92**, 75.
- J. Sikora, M. Pado, M. Tatarko, and M. Izakovic, *J. Photochem. Photobiol. A: Chem.*, 1997, **110**, 167.
- J. Chen, L. Eberlein, and C. H. Langford, *J. Photochem. Photobiol. A: Chem.*, 2002, **148**, 183.
- C. Liu, X. Ye, R. Zhan, and Y. Wu, *J. Molecular Catalysis A: Chem.*, 1996, **112**, 15.
- G. Stein and J. Weiss, *J. Chem. Soc.*, 1951, 3265.
- Al-Ajlouni, A. Bakac, and J. H. Espenson, *Inorg. Chem.*, 1993, **32**, 5792.
- H. Huang, D. Sommerfeld, B. C. Dunn, E. M. Eyring, and C. R. Lloyd, *J. Phys. Chem.*, 2001, **105**, 3536.
- N. Kitajima, T. Koda, Y. Iwata, and Y. Moro-oka, *J. Am. Chem. Soc.*, 1990, **112**, 8833.
- A. Nemes and A. Bakac, *Inorg. Chem.*, 2001, **40**, 746.
- R. Gupta and R. Mukherjee, *Tetrahedron Lett.*, 2000, **41**, 7763.
- E. J. Land, *J. Chem. Soc., Faraday Trans.*, 1993, **89**, 803.

Received May 17, 2004